

Design and Optimization of Tricyclic Phthalimide Analogues as Novel Inhibitors of HIV-1 Integrase

Wim G. Verschuereen,^{*,†} Inge Dierynck,[†] Katie I. E. Amssoms,[†] Lili Hu,[†] Paul M. J. G. Boonants,[†] Geert M. E. Pille,[†] Frits F. D. Daeyaert,[‡] Kurt Hertogs,[†] Dominique L. N. G. Surleraux,[†] and Piet B. T. P. Wigerinck[†]

Tibotec BVBA, Generaal de Wittelaan L 11B 3, B-2800 Mechelen, Belgium, and Center for Molecular Design, Johnson & Johnson Pharmaceutical Research & Development, Antwerpsesteenweg 37, B-2350 Vosselaar, Belgium

Received June 7, 2004

Human immunodeficiency virus type-1 integrase is an essential enzyme for effective viral replication and hence a valid target for the design of inhibitors. We report here on the design and synthesis of a novel series of phthalimide analogues as integrase inhibitors. The short synthetic pathway enabled us to synthesize a series of analogues with a defined structure diversity. The presence of a single carbonyl–hydroxy–aromatic nitrogen motif was shown to be essential for the enzymatic activity and this was confirmed by molecular docking studies. The enzymatically most active compound from this series is 7-(3,4-dichlorobenzyl)-5,9-dihydroxypyrrulo[3,4-g]quinoxaline-6,8-dione (**15l**) with an IC₅₀ value of 112 nM on the HIV-1 integrase enzyme, while ((7-(4-chlorobenzyl)-5,9-dihydroxy-pyrrolo[3,4-g]quinoxaline-6,8-dione (**15k**)) showed an EC₅₀ of 270 nM against HIV-1 in a cell-based assay.

Introduction

Since 1981, acquired immunodeficiency syndrome or AIDS has become a major worldwide epidemic. AIDS is caused by human immunodeficiency virus (HIV). By killing or damaging cells of the immune system, HIV progressively destroys the body's ability to withstand infections and certain cancers. Looking at the life cycle of this retrovirus, three essential enzymes, encoded by the HIV *pol* gene can be distinguished: (i) reverse transcriptase, (ii) integrase, and (iii) protease.¹ Reverse transcriptase is an RNA/DNA-dependent DNA polymerase that transcribes the viral genomic RNA into proviral DNA. Integrase then associates with a series of cellular factors and the proviral DNA to form the preintegration complex (PIC). The complex migrates to the nucleus, where integration takes place, involving, for example, cleavage of two nucleotides from each 3'-terminal of the proviral DNA and the strand transfer reaction, both catalyzed by the viral enzyme. This process is essential for viral replication and hence a valid target for the design of inhibitors. As of today, whereas integrase inhibitors have been identified, which inhibit both the viral enzyme and the virus replication in cell-based assays as well in animal models, no inhibitor of HIV integrase has been approved yet.²

The HIV-1 protease (PR) hydrolyzes viral polyproteins into functional protein or peptide products that are essential for viral assembly and subsequent replication. Various protease and reverse transcriptase inhibitors are currently available as approved antiretroviral drugs; however, their suboptimal use associated with the high mutation rate of HIV have rendered those drugs of very limited use for a large proportion of patients, due to viral resistance to these inhibitors.

There is therefore a high unmet need for drugs with new mechanisms of action, which are not limited by existing drug resistance, to combat the HIV-1 infection. Recently, a large interest in HIV integrase has emerged. This enzyme is an attractive target for anti-HIV drug discovery and development because it is essential to the viral life cycle and is absent in the host cell.^{3–5}

Molecular Modeling

Structure-based drug-design efforts on HIV integrase have been hampered by the lack of structural information on the exact binding mode of known inhibitors. One structure of an inhibitor cocrystallized with the core domain of HIV integrase has been published.⁶ We and others,^{7,8} however, believe that the observed binding position of the inhibitor in this crystal structure is influenced by crystal packing effects and does not reflect the binding mode in an active biological system. Various reported QSAR studies on different series of integrase inhibitors using methods that do not require structural information about the target enzyme have been published.^{9–12} The picture that emerges from those efforts is that different classes of inhibitors seem to have different mechanisms of action.¹³ For a subset of these classes, we have hypothesized, using the structural information from crystal structures of the core domain of HIV integrase complexed to Mg²⁺, a binding mode based on the presence of a metal chelating pharmacophore.^{14,15}

HIV integrase consists of three distinct domains: the N-terminal domain, the catalytic core domain, and the C-terminal domain. X-ray and/or NMR structures of the separate subdomains and of the core domains with the N-terminal and C-terminal domains have been published.^{14–24} The catalytic core domain comprises the residues 51–212. This domain contains two aspartates and one glutamate (Asp64, Asp116, and Glu152, the "D,D(35),E" motif) that are essential for catalytic activity of various DNAses and are believed to bind Mg²⁺ or

* To whom correspondence should be addressed. Phone: +32 (0)15293178. Fax: +32 (0)15401257. E-mail: wversch1@tibbe.jnj.com.

[†] Tibotec BVBA.

[‡] Johnson & Johnson Pharmaceutical Research & Development.

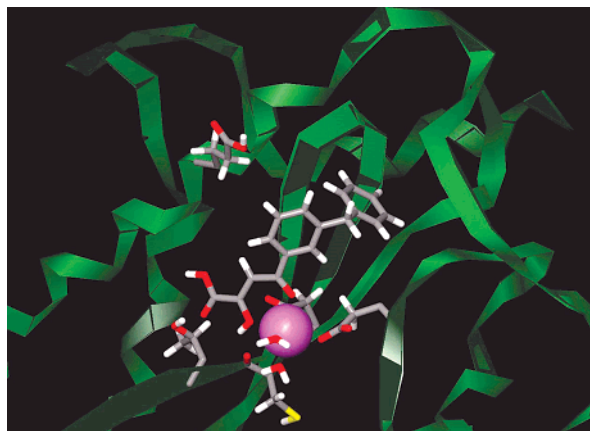


Figure 1. Proposed binding mode of diketo acid **1**²⁸ into the core domain of HIV-1 integrase. The Mg^{2+} ion is cpk rendered. The inhibitor, the amino acid side chains of Asp64, Asp116, Glu152, Thr66, and Cys65, and the two water molecules completing the Mg^{2+} coordination are rendered in stick.

Mn^{2+} . The presence of either of these divalent ions is required for HIV integrase catalytic activity. Also, the binding and activity of integrase inhibitors is metal dependent.^{25–27} In two X-ray structures of the core domain, a single Mg^{2+} ion is chelated by Asp64 and Asp116.^{14,15} We propose a binding mode in which inhibitors bind through bidentate chelation of this ion. To determine the orientation of a bidentate integrase inhibitor in the integrase enzyme, we carried out manual docking studies using the diketo acid **1** (see Figure 1). This compound was the most active in a series of compounds where the angle formed by the lines extended from the diketo acid and benzyl groups toward the central aromatic ring was varied by structurally altering this central ring.²⁸ Given the chelation of the Mg^{2+} by the aspartates 64 and 116 and the octahedral coordination of Mg^{2+} , there are a limited number of ways (10, see the Experimental Section) to complete this coordination with a bidentate ligand. The configuration with the lowest ligand–enzyme nonbond interaction energy is shown in Figure 1. In this orientation, the benzyl group makes a turn inward to the protein, filling a hydrophobic pocket formed in part by the flexible outer loop of the integrase core domain. It has been shown that this loop is important for enzymatic activity.²² The acid group acts as a hydrogen-bond acceptor to the hydroxy group of ThrA66, while the enol hydrogen forms a hydrogen bond toward the carbonyl oxygen of Cys65. Interestingly, it has been described that HIV-1 grown in the presence of the diketo acid inhibitor L-708,906 developed resistance as the result of mutations of ThrA66.²⁹ Starting from the proposed integrase–inhibitor complex shown in Figure 1,³⁰ we have developed the following protocol for docking putative HIV-1 integrase inhibitors.

First, a conformational analysis of the ligand is carried out using a genetic algorithm (GA). The outcome of this GA is a list of fully molecular mechanics optimized low-energy conformers. The parameters of the GA have been fine-tuned such that in several runs using different initial configurations, the same low-energy conformations are consistently generated.

For each conformer, all possible bidentate complexes with a Mg^{2+} ion are formed by placing a Mg^{2+} ion

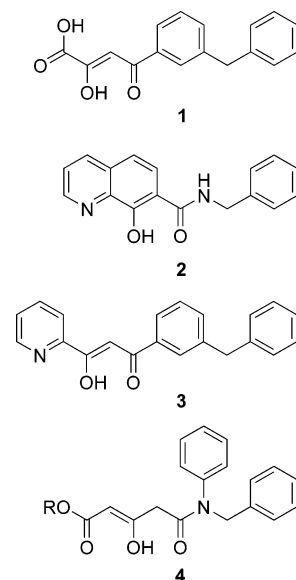


Figure 2. Various classes of compounds that can be docked into the core domain of HIV-1 integrase using the proposed docking protocol: **1**, diketo acids;²⁶ **2**, naphthyridines;²⁹ **3**, 1,3-diketones;²⁹ **4**, β -keto amides.³⁰

between each pair of possible coordinating atoms of the ligand. For the diketo acid in Figure 1, these are between the keto and enol or between the enol and carbonyl acid oxygens. For the phthalimide compounds these are between the carbonyl and hydroxyl and between the hydroxyl and the pyrazine nitrogens. All bidentate chelates are subjected to molecular mechanics minimization.

The Mg^{2+} –ligand chelates are then superimposed upon the coordinates of the Mg^{2+} and the two removed water molecules in the integrase active site structural model.³¹ This superposition is carried out using Kabsch' algorithm for the superposition of two vectors. As the coordinating atoms are equivalent, this can be done in two ways. For each pose, the nonbond interaction between the chelate and the integrase enzyme is calculated using a precalculated grid.

The chelate–enzyme complexes with the lowest nonbond interaction energy calculated in the previous step are subjected to full molecular mechanics energy minimization. The complex with the lowest chelate–enzyme interaction energy after this final minimization is retained as the final docking result.

The force field used in the molecular mechanics calculations is an in-house adapted version of MMFF94.³² The nonbond interaction grid is calculated using a 4–8 Lennard-Jones-type potential fitted to the original 7–14 functional form. The 4–8 functional form is used as it has been documented that the use of softer potentials improves existing docking algorithms.³³ The fast nonbond energy calculation using the precalculated grids is used to select low-energy chelate–enzymes, which can then be subjected to the computationally much more expensive full molecular mechanics minimization. To reduce the computational time, only five chelate–enzyme complexes are minimized.

With this docking protocol, various classes of HIV integrase inhibitors can be docked in a consistent way. Examples include the diketo acids **1**, naphthyridines **2**, 1–3 diketones **3**, and β -keto amides **4** (see Figure 2).^{34,35}

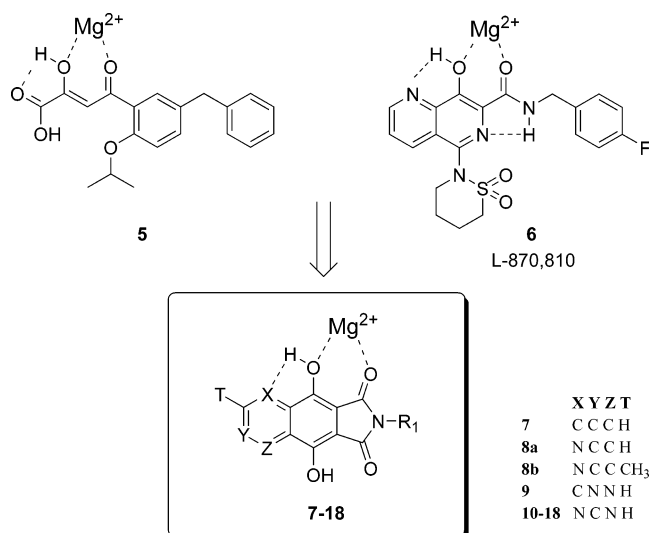
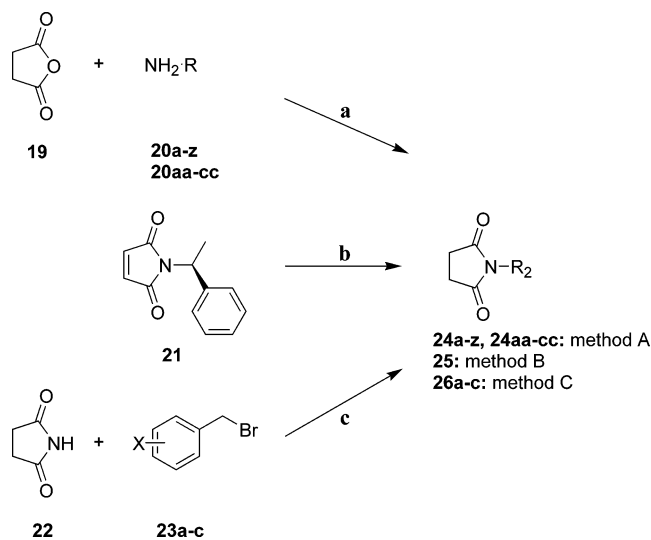


Figure 3. Design of tricyclic phthalimide analogues 7–18.

Scheme 1. Synthesis of 1-Substituted Pyrrolidine-2,5-dione Analogues **24a–z**, **24aa–cc**, **25**, and **26a–c**^a



^a Reagents and conditions: (a) DMAP, HOAc, reflux, 2–72 h; (b) 10% Pd/C–H₂, CH₃OH, rt, 24 h; (c) K₂CO₃, 18-crown-6, CH₃CN, reflux, 24 h.

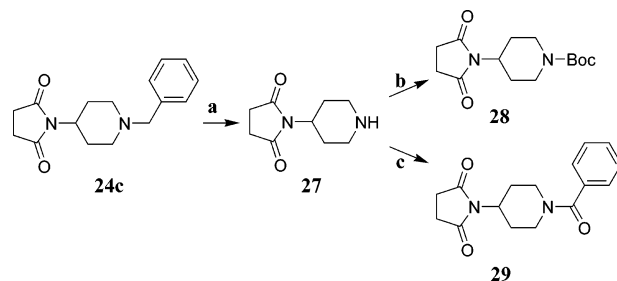
This information, together with the diketo acid moiety present in compound **5** and the motif present in the azanaphthyridine analogue **6** (L-870,810), both described by Pais et al., were used to design and synthesize a novel series of phthalimide analogues as candidate integrase inhibitors (see Figure 3).³⁶

In this paper we report the systematic search for new, potent, and selective integrase inhibitors. The structure–activity relationship of several classes of phthalimide analogues as integrase inhibitors was investigated.

Chemistry

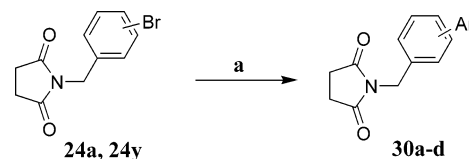
The general synthetic route we applied for the synthesis of the tricyclic phthalimide analogues **7–18** is summarized in Schemes 1–4. In Scheme 1 we describe three different approaches to synthesize the 1-substituted-pyrrolidine-2,5-dione analogues **24a–z**, **24aa–cc**, **25**, and **26a–c**. Method A starts from dihydrofuran-2,5-dione (**19**), which reacted with different amines

Scheme 2. Synthesis of 1-Substituted Piperidin-4-ylpyrrolidine-2,5-dione Analogues **27–29**^a



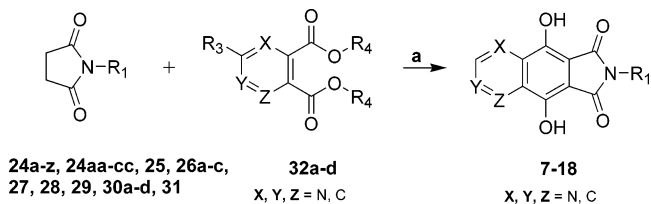
^a Reagents and conditions: (a) 10% Pd/C–H₂, CH₃OH, rt, 24 h; (b) Boc₂O, CH₂Cl₂, rt, 24 h; (c) benzoyl chloride, Na₂CO₃, THF–H₂O (1:1), rt, 24 h.

Scheme 3. Synthesis of 1-Substituted-pyrrolidine-2,5-dione Analogues **30a–d**^a



^a Reagents and conditions: (a) boronic acid, Pd(OAc)₂, NaTM-SPP, Et₃N, THF–H₂O (1:1), reflux, 0.5–24 h.

Scheme 4. Synthesis of Tricyclic Phthalimide Analogues **7–18**^a



^a Reagents and conditions: (a) NaH, CH₃OH (catalytic amount), THF, reflux, 48 h.

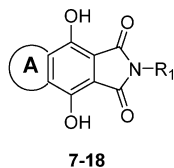
20a–z, **20aa–cc** in acetic acid as a solvent and a catalytic amount of DMAP to yield the different pyrrolidine-2,5-dione analogues **24a–z**, **24aa–cc**. Hydrogenation of the commercially available 1-[(1*R*)-1-phenylethyl]pyrrolidine-2,5-dione (**21**) gave the analogue **25** as described in method B. Method C consists of a nucleophilic substitution between pyrrolidine-2,5-dione (**22**) and the substituted benzyl bromide analogue **23a–c** in the presence of potassium carbonate as a base.

Debenzylation of the **24c** 1-(1-benzylpiperidin-4-yl)pyrrolidine-2,5-dione yielded the deprotected piperidine analogue **27** (Scheme 2). The secondary amine was protected as a carbamate with di-*tert*-butyl dicarbonate in dichloromethane to give the carbamoylated pyrrolidine-2,5-dione **28**. In route C, the amine function of **27** was acylated with benzoyl chloride in tetrahydrofuran:water (1:1) by applying sodium carbonate as a base.

Compounds **30a–d** were achieved via a Suzuki coupling, in the presence of palladium acetate, triphenylphosphine-3,3',3''-trisulfonic acid trisodium salt (Na TMSPP) as a water-soluble ligand, a boronic acid derivative, and triethylamine (Et₃N) as a base as described in Scheme 3.

The tricyclic phthalimide analogues **7–18** (Scheme 4) were synthesized via a double Claisen condensation of an appropriately *N*-substituted succinimide **24a–z**, **24aa–cc**, **25**, **26a–c**, **27**, **28**, **29**, **30a–d**, and **31** with

Table 1. Biochemical and Biological Evaluation of Tricyclic Phtalimide Analogues 7–18



Compound type	ring A	R ₁	pIC ₅₀ ^a	pEC ₅₀ ^a	pCC ₅₀ ^a
7			< 4.00	4.70	4.59
8a			6.42	5.51	5.21
8b			6.59	5.12 ± 0.41	4.78 ± 0.10
9			5.44	4.67 ± 0.16	< 4.49
10			6.68	5.13 ± 1.83	4.49 ± 0.45
11a		—CH ₃	4.31	< 4.49	< 4.49
11b			4.98	< 4.49	4.55
11c			< 4.00	< 4.49	< 4.49
11d			5.62	< 4.49	< 4.49
11e			5.66	5.46 ± 0.09	5.19 ± 0.08
12a			5.98 ± 0.21	4.99 ± 0.39	4.76 ± 0.04
12b			5.69	4.82 ± 0.01	4.81 ± 0.04
13a			5.00	< 4.49	< 4.49
13b			6.25 ± 0.38	5.50 ± 0.52	< 4.49

Table 1 (Continued)

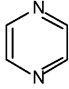
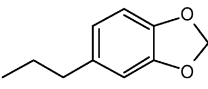
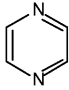
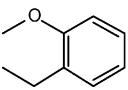
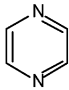
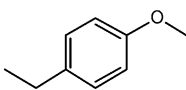
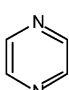
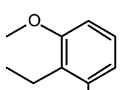
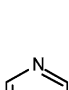
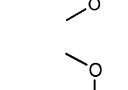
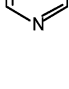
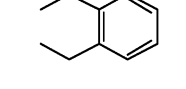
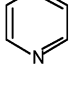
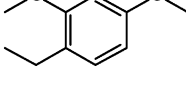
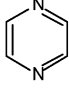
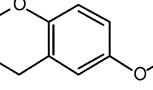
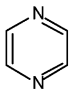
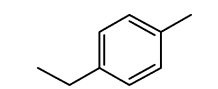
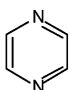
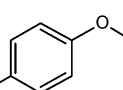
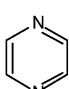
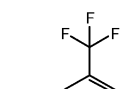
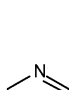
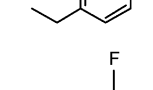
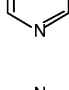
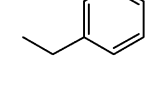
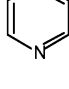
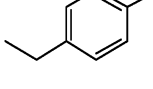
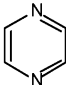
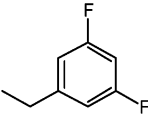
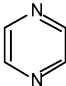
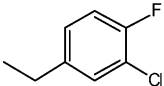
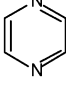
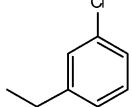
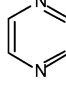
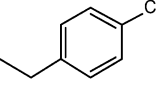
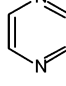
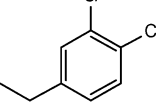
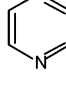
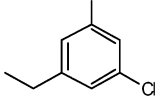
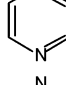
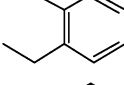
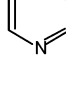
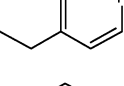
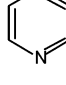
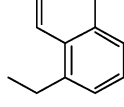
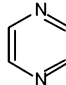
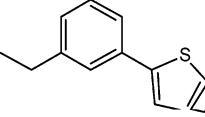
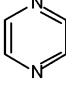
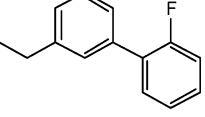
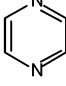
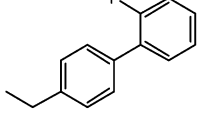
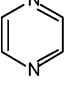
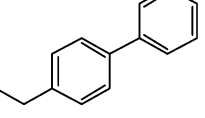
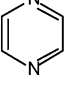
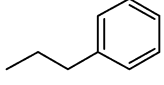
Compound type	ring A	R ₁	pIC ₅₀ ^a	pEC ₅₀ ^a	pCC ₅₀ ^a
13c			5.85	4.96 ± 0.12	ND
14a			6.09 ± 0.18	5.42 ± 0.35	4.81 ± 0.04
14b			6.25	5.44	4.64
14c			5.70 ± 0.14	5.27 ± 0.14	5.09 ± 0.29
14d			6.37	5.31	4.72
14e			6.37	4.87	4.77
14f			6.11 ± 0.15	5.32 ± 0.08	4.73
15a			5.80	5.75	4.86
15b			5.69	5.87	5.60
15c			6.37	5.01	4.77
15d			6.25	5.27	4.77
15e			6.38 ± 0.19	5.81 ± 0.53	4.69 ± 0.10
15f			6.36	5.62	5.11
15g			6.45	6.35	5.38

Table 1 (Continued)

Compound type	ring A	R ₁	pIC ₅₀ ^a	pEC ₅₀ ^a	pCC ₅₀ ^a
15h			6.43 ± 0.32	4.78 ± 0.42	< 4.49
15i			6.75 ± 0.46	5.51 ± 0.02	4.70 ± 0.28
15j			6.66 ± 0.09	6.01	4.73 ± 0.02
15k			6.38	6.57	5.58
15l			6.95 ± 0.29	6.04 ± 0.12	5.05 ± 0.17
15m			6.73 ± 0.33	6.14 ± 0.01	4.72 ± 0.10
15n			6.20	4.82	4.75
16			5.17	< 4.49	< 4.49
17a			5.85	5.34 ± 0.04	ND
17b			6.17	4.93	4.78
17c			6.30	4.88	4.82
17d			6.00	4.83	4.83
17e			5.84	5.59	5.47
18			5.69	5.31	5.23

^a The standard deviation is given for experiments where the number of determinations is more than two. All the determinations are quadruplet values. ND = not determined. ^b The reference compounds (**5**, **6**) have an IC₅₀ of 0.05 and 0.01 μM, respectively, and an EC₉₅ value of 0.10 μM.³⁴

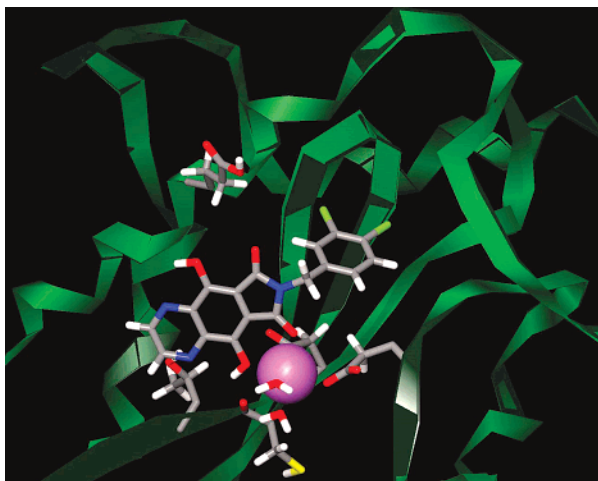


Figure 4. Compound **151** docked into the core domain of HIV-1 integrase.

the aromatic ortho diester **32a–d**³⁷ in tetrahydrofuran solution and sodium hydride as base in the presence of a catalytic amount of methanol as described by Murray et al.³⁸ The yields and the different types of compounds that were synthesized are given in Table 1.

Results and Discussion

Molecular Modeling. The proposed binding hypothesis, based on the presence of a metal-chelating pharmacophore, and docking analysis procedure have been helpful in the optimization of the present class of tricyclic phthalimide analogues derived from compound **10**. Figure 4 shows the result of the docking of compound **151**, one of the more potent analogues, into the integrase core domain using the above-described docking protocol. The carbonyl and hydroxy oxygens chelate the Mg^{2+} ion in the active site. The Asp64 and Asp116 acid side chains and two water molecules complete the octahedral coordination sphere of the ion. Important interactions with the enzyme are hydrogen bonds (i) between the left pyrazine nitrogen and the hydroxy group of Thr66 and (ii) between the enol hydrogen and the backbone carbonyl of Cys65 and (iii) the hydrophobic interaction of the benzyl substituent with the flexible loop formed by residues 140–148. Most phthalimide analogues can be consistently docked in this binding mode using the proposed docking protocol. Exceptions are compounds with larger substituents on the phthalimide moiety, like **17a**, **17b**, and **17c**. A number of SAR observations can be rationalized with the aid of the proposed binding model. The presence of a single carbonyl–hydroxy–aromatic nitrogen motif is essential for activity. However, only one such motif is necessary, as demonstrated in the activities of compounds such as **8a** and **9**. Also important is the “turn” in the molecules to direct the hydrophobic substituent on the phthalimide nitrogen toward the flexible loop. This is illustrated by the lower antiviral activity of compounds **11a**, **11b**, **11c**, and **13a**.

Inhibitory Properties of a Series of Tricyclic Phthalimide Analogues 7–18. All the compounds were tested for their ability to inhibit the HIV-1 virus. All the data are shown in Table 1. Compounds **5** and **6** described by Pais et al. are shown for comparison, because of their known ability to inhibit HIV-1 integra-

tion in vitro.^{36,39} Several phthalimides were synthesized in order to explore the aryl- and R-moieties. One of the first compounds synthesized in this series was compound **7** (2-(4-fluorobenzyl)-4,9-dihydroxybenzo[*f*]isoin-dole-1,3-dione) with a phenyl ring on the left. The inactivity of compound **7** showed that a hydrogen-bond acceptor adjacent to the phenol function was essential in comparison with the pyrazine analogue **10** ($pIC_{50} = 6.68$). The pyrazine ring was kept constant in a series of R1-variations. The important carbonyl–hydroxy–aromatic nitrogen motif is present twice in this molecule. In the series of benzodioxole derivatives the spacer length was explored ($n = 1–3$). The optimal chain length is 1, as was shown by compound **13b** with a pIC_{50} value of 6.25. This is consistent with the ability to direct the hydrophobic substituents toward the flexible loop of HIV-integrase. A set of mono- and dimethoxybenzyl derivatives was synthesized **14a–f**. These derivatives showed similar results, except the 2,6-dimethoxybenzyl analogue **14c**, with a 0.5 log reduced activity on HIV-integrase, and the 2,4-dimethoxybenzyl derivative **14e**, which in this series is clearly the least active compound in the cell-based anti-HIV assay, having a pEC_{50} value of 4.87. Some alkyl analogues, **11a–e** and **12a–b**, were made but showed reduced activity on the enzyme and no activity in cell culture except the cyclohexylmethyl derivative **11e** ($pEC_{50} = 5.46$). The two enantiomers of the α -methylbenzyl substituted compounds **12a–b** were toxic. The pyridine analogue **16** lost 1 log of enzymatic activity ($pIC_{50} = 5.17$) in comparison with the benzodioxole derivative **13b** and was not active in the cell-based anti-HIV assay. A few aryl- and phenyl-substituted benzyl derivatives were made (**17a–e**). Compound **17e** was the most interesting compound of this series: this more lipophilic compound was less active on the enzyme but showed a comparable activity with **13b** in the cell-based anti-HIV assay. Another series of methyl, trifluoromethyl, trifluoromethoxy, and halogenated benzyl derivatives **15a–n** and **10** were synthesized. The monohalogenated (F, Cl, Br) compounds showed a similar enzymatic activity with a pIC_{50} of 6.5, while compound **15k** was clearly better in the cell-based anti-HIV assay, where a pEC_{50} of 6.57 was measured. In the dihalogenated benzyl derivatives series, the chloro-substituted analogues showed a superior activity, which was illustrated by the 3,4-dichlorobenzyl (**15l**) ($pIC_{50} = 6.95$ and $pEC_{50} = 6.04$) and the 3,5-dichlorobenzyl (**15m**) ($pIC_{50} = 6.73$ and $pEC_{50} = 6.14$) analogues. One of the most active compounds was the *m*-bromobenzyl derivative **10**, which showed a pIC_{50} of 6.68. This *m*-bromobenzyl substituent was chosen to explore the aromatic moiety on the “left” part of the molecule. The pyridine **8a** and methylpyridine **8b** showed similar activities.

All the tricyclic phthalimide analogues demonstrated a similar activity on the enzyme when compared with the naphthyridine analogue **6** described by Pais et al. but were less selective.³⁶

Conclusion

The design and synthesis of tricyclic phthalimides analogues resulted in a new class of HIV-1 integrase inhibitors. The short synthetic pathway allowed us to synthesize a series of phthalimide analogues with a

defined structure diversity. Essential structural features, including the carbonyl–hydroxy–aromatic nitrogen motif, for the enzymatic activity were confirmed. The enzymatically most active compound from this series is **15l** with an IC₅₀ value of 112 nM on the HIV-1 integrase enzyme, while [(7-(4-chlorobenzyl)-5,9-dihydroxypyrrolo[3,4-g]quinoxaline-6,8-dione (**15k**)] showed an EC₅₀ of 270 nM against HIV-1 in a cell-based assay. Further research is ongoing to increase the cell penetration and selectivity of these tricyclic phthalimide series.

Experimental Section

General Experimental Procedures. NMR spectra were recorded, using standard software packages, on a Bruker Avance 400 spectrometer, operating at 400 MHz for ¹H and 100 MHz for ¹³C and with DMSO or CDCl₃ as solvent unless otherwise stated. In every case tetramethylsilane (TMS) was used as internal standard. Chemical shifts are given in ppm and *J* values in Hz. Multiplicity is indicated using the following abbreviations: d for a doublet, t for a triplet, m for a multiplet, etc. An additional 2-D measurement (HSQC) was performed for complete structure elucidation of the tricyclic phthalimide analogues. With this measurement, it was proven that the benzylic CH₂ for the different tricyclic phthalimide analogues has a value of 39.9 ppm unless otherwise stated. For the sake of brevity, we opted to completely characterize (NMR included) one representative example of each subset of final products **7–18**. Low-resolution mass spectra (LRMS) were collected on a single quadrupole mass spectrometer (Waters ZMD), with ion trap (ThermoFinnigan LCQ Deca) or time-of-flight (Waters LCT) using electrospray ionization (ESI) in positive or negative mode.

All reagents were purchased from commercial sources (Acros, Aldrich, ABCR, etc.) and were used as such. Column chromatography was carried out on silica gel 60 Å, 60–200 μm (ROCC). Thin-layer chromatography was performed on silica gel 60 F₂₅₄ plates (Merck). Analytical HPLC was done on a Waters Alliance 2690 (pump + autosampler) system equipped with a Waters 996 photodiode array-detector. The purity of the final compounds **7–18** was determined with three HPLC systems using a UV-detector: In system 1, a Waters Xterra MS C18 column (3.5 μm, 4.60 mm × 100 mm) was used and the UV detection range was set at 230–300 nm. In system 2, a Thermo Hypersil BDS C18 column (3.5 μm, 4 mm × 100 mm) was used and a single wavelength (λ_{max}) was set. In system 3, an Alltech Prevail C18 column (3 μm, 4 mm × 100 mm) was used and a single wavelength (λ_{max}) was set. The applied gradient was the same for systems 1 and 2: 10 mM ammonium formate and 0.1% formic acid in water (mobile phase A) and acetonitrile (mobile phase B), with a gradient from 5% to 95% acetonitrile in 12 min. The applied gradient for system 3 was 0.1% trifluoroacetic acid in water (mobile phase A) and acetonitrile (mobile phase B), with a gradient from 0% to 95% acetonitrile in 12 min. The flow rate was 1.0 mL/min for the three systems. The retention time of each compound in both systems is given in minutes. Elemental analyses were performed on a Carlo-Erba EA1110 analyzer. The coulometric Karl Fisher method was used for water determination.

General Reaction Procedure 1. Representative Procedures for the Synthesis of 1-Substituted Pyrrolidine-2,5-dione Analogues 24a–z, 24aa–cc, 25, and 26a–c. Method A: Representative Procedure for the Synthesis of 1-Substituted Pyrrolidine-2,5-dione Analogues 24a–z and 24aa–cc. Synthesis of 1-(3-Bromobenzyl)pyrrolidine-2,5-dione (**19**). Dihydrofuran-2,5-dione (**1**) (1.00 g, 0.01 mol) and 3-bromobenzylamine (**20a–z**, **20aa–cc**) (1.86 g, 0.01 mol) were dissolved in acetic acid (25 mL), followed by the addition of a catalytic amount of dimethylpyridin-4-ylamine (DMAP). The solution was refluxed for 24 h. After completion of the reaction, the solution was cooled to room temperature. The solvent was removed under reduced pressure and the residue was dissolved

in dichloromethane (50 mL). The organic layer was washed with saturated NaHCO₃ solution (50 mL) and 1 N HCl solution. The organic layer was dried over magnesium sulfate and evaporated under reduced pressure to yield the title compound as a white crystalline product (1.75 g, 65%).

The following products (**24b–z**, **24aa–cc**) were prepared in this manner; the yields and different reaction times are mentioned for each product. All the products were identified by LRMS, and a few representative compounds were characterized by ¹H NMR and ¹³C NMR spectra (see the Supporting Information).

- 1-Cyclopentylpyrrolidine-2,5-dione (**24b**): 69% yield.
- 1-(1-Benzylpiperidin-4-yl)pyrrolidine-2,5-dione (**24c**): 80% yield.
- 1-[(1S)-1-Phenylethyl]pyrrolidine-2,5-dione (**24d**): 86% yield, 72 h.
- 1-Benzo[1,3]dioxol-5-ylpyrrolidine-2,5-dione (**24e**): 93% yield.
- 1-Benzo[1,3]dioxol-5-ylmethylpyrrolidine-2,5-dione (**24f**): 87% yield, 72 h.
- 1-(2-Benzo[1,3]dioxol-5-ylethyl)pyrrolidine-2,5-dione (**24g**): 100% yield.
- 1-(2-Methoxybenzyl)pyrrolidine-2,5-dione (**24h**): 83% yield.
- 1-(4-Methoxybenzyl)pyrrolidine-2,5-dione (**24i**): 74% yield, 72 h.
- 1-(2,6-Dimethoxybenzyl)pyrrolidine-2,5-dione (**24j**): 79% yield.
- 1-(2,3-Dimethoxybenzyl)pyrrolidine-2,5-dione (**24k**): 70% yield, 2 h.
- 1-(2,4-Dimethoxybenzyl)pyrrolidine-2,5-dione (**24l**): 75% yield, 2 h.
- 1-(2,5-Dimethoxybenzyl)pyrrolidine-2,5-dione (**24m**): 81% yield.
- 1-(4-Methylbenzyl)pyrrolidine-2,5-dione (**24n**): 92% yield.
- 1-(4-Trifluoromethoxybenzyl)pyrrolidine-2,5-dione (**24o**): 85% yield.
- 1-(3-Fluorobenzyl)pyrrolidine-2,5-dione (**24p**): 64% yield, 72 h.
- 1-(4-Fluorobenzyl)pyrrolidine-2,5-dione (**24q**): 91% yield.
- 1-(4-Bromo-2-fluorobenzyl)pyrrolidine-2,5-dione (**24r**): 75% yield.
- 1-(2-Bromo-6-fluorobenzyl)pyrrolidine-2,5-dione (**24s**): 83% yield.
- 1-(3-Chlorobenzyl)pyrrolidine-2,5-dione (**24t**): 70% yield.
- 1-(4-Chlorobenzyl)pyrrolidine-2,5-dione (**24u**): 70% yield.
- 1-(3,4-Dichlorobenzyl)pyrrolidine-2,5-dione (**24v**): 68% yield.
- 1-(3,5-Dichlorobenzyl)pyrrolidine-2,5-dione (**24w**): 55% yield.
- 1-(2-Bromobenzyl)pyrrolidine-2,5-dione (**24x**): 61% yield.
- 1-(4-Bromobenzyl)pyrrolidine-2,5-dione (**24y**): 48% yield.
- 1-Cyclohexylmethylpyrrolidine-2,5-dione (**24z**): 82% yield, 72 h.
- 1-Pyridin-4-ylmethylpyrrolidine-2,5-dione (**24aa**): 75% yield.
- 1-Naphthalen-2-ylmethylpyrrolidine-2,5-dione (**24bb**): 98% yield.
- 1-[(1S)-1-Phenethyl]pyrrolidine-2,5-dione (**24cc**): 99% yield.

Method B. Synthesis of 1-[(1R)-1-Phenylethyl]pyrrolidine-2,5-dione (25). After displacing the air with N₂, palladium on charcoal (10%, 0.30 g) was added followed by the addition of a solution of 1-[(1R)-1-phenylethyl]pyrrolidine-2,5-dione (1 g, 4.97 mmol) (**21**) in methanol (100 mL). For a few minutes vacuum was applied and replaced by H₂. After stirring for 24 h at room temperature, N₂ was then introduced in the flask to displace the remaining H₂. The palladium catalyst was removed by filtration over a bed of Celite under N₂ and the filter was washed with methanol. The filtrate was evaporated under reduced pressure (1.01 g, 100%).

Method C. Representative Procedure for the Synthesis of 1-Substituted Pyrrolidine-2,5-dione Analogues 26a–c. Synthesis of 1-(3-Trifluoromethylbenzyl)pyrrolidine-2,5-dione (26a). Pyrrolidine-2,5-dione (2.30 g, 23.22 mmol) (**22**), 1-bromomethyl-3-trifluoromethyl-benzene (5.05 g, 21.11 mmol) (**23a–c**), K₂CO₃ (6.18 g, 49.83 g), and 18-crown-6 (0.10 g) were dissolved in acetonitrile (100 mL). The solution was refluxed for 24 h. The solution was concentrated and the residue was purified by column chromatography on elution

with dichloromethane (4.34 g, 80%) to yield the title compound as a white crystalline product.

The following products were prepared in the same manner: 1-(3,5-Difluorobenzyl)pyrrolidine-2,5-dione (**26b**) and 1-(3-chloro-4-fluorobenzyl)pyrrolidine-2,5-dione (**26c**).

Preparation of 1-Substituted Piperidin-4-ylpyrrolidine-2,5-dione Analogues (27–29). Method A: Synthesis of 1-Piperidin-4-ylmethylpyrrolidine-2,5-dione (27). The removal of the benzyl moiety of 1-(1-benzylpiperidin-4-yl)pyrrolidine-2,5-dione (**24c**) (12.20 g, 45.19 mmol) was done with palladium on charcoal and hydrogen as previously described (8.13 g, 100%).

Method B: Synthesis of 4-(2,5-Dioxypyrrolidin-1-ylmethyl)piperidine-1-carboxylic Acid *tert*-Butyl Ester (28). 1-Piperidin-4-ylmethylpyrrolidine-2,5-dione (**27**) (1.96 g, 10.73 mmol) and di-*tert*-butyl dicarbonate (2.48 g, 11.35 mmol) were dissolved in dichloromethane (50 mL). The solution was stirred at room temperature for 24 h. The solution was concentrated and coevaporated with toluene (3.02 g, 100%).

Method C: Synthesis of 1-(1-Benzoylpiperidin-4-ylmethyl)pyrrolidine-2,5-dione (29). 1-Piperidin-4-ylmethylpyrrolidine-2,5-dione (**27**) (1 g, 3.38 mmol), benzoyl chloride (0.47 g, 3.38 mmol), and Na₂CO₃ (0.36 g, 3.38 mmol) were dissolved in a mixture of tetrahydrofuran:water (1:1) (30 mL). The solution was stirred at room temperature for 24 h. After completion of the reaction, the organic layer was separated and concentrated. The organic layer was washed with 1 N HCl solution (2 × 40 mL), dried over magnesium sulfate, and evaporated under reduced pressure to yield the title compound **29**.

General Reaction Procedure 2. Representative Procedure for the Synthesis of 1-Substituted Pyrrolidine-2,5-dione Analogues 30a–d. Method A: Synthesis of 1-(3-Thiophen-2-ylbenzyl)pyrrolidine-2,5-dione (30a). 1-(3-Bromobenzyl)pyrrolidine-2,5-dione (**24a**) (method A, general reaction procedure 1) (0.54 g, 2 mmol), thiopheneboronic acid (0.26 g, 2 mmol), palladium acetate (22.50 mg, 0.10 mmol), triphenylphosphine-3,3',3''-trisulfonic acid trisodium salt (Na TMSPP) (0.11 g, 0.20 mmol), and triethylamine (1.01 g, 10 mmol) were dissolved in a mixture of tetrahydrofuran:water (1:1) (30 mL). The solution was refluxed for 30 min. The solution was cooled to room temperature and the organic layer was separated. The organic layer was concentrated, dissolved in dichloromethane (30 mL), and washed with 10% citric acid solution (30 mL). The organic layer was dried over magnesium sulfate and evaporated under reduced pressure to yield the title compound **30a** (0.31 g, 57%).

The following products were prepared in the same manner.

1-Biphenyl-4-ylmethylpyrrolidine-2,5-dione (**30b**): 58% yield, 24 h.

1-(2'-Fluorobiphenyl-3-ylmethyl)pyrrolidine-2,5-dione (**30c**): 76% yield, 24 h.

1-(2'-Fluorobiphenyl-4-ylmethyl)pyrrolidine-2,5-dione (**30d**): 56% yield, 24 h.

1-Methylpyrrolidine-2,5-dione (**31**) was purchased from Aldrich.

General Reaction Procedure 3. Representative Procedure for the Preparation of Phthalimide Analogues (7–18).³³ Method A. Synthesis of 7-(3-bromobenzyl)-5,9-dihydroxy-pyrrolo[3,4-g]quinoline-6,8-dione (8a). Pyridine-2,3-dicarboxylic acid dimethyl ester (0.20 g, 1.04 mmol) (**32a**) and 1-(3-bromobenzyl)pyrrolidine-2,5-dione (0.28 g, 1.04 mmol) (**24a**) were dissolved in tetrahydrofuran (30 mL), followed by the addition of sodium hydride (0.17 g, 4.16 mmol) and methanol (catalytic). The solution was refluxed for 48 h. The solution was cooled to room temperature and concentrated. The residue was suspended in water. The aqueous solution was acidified with 12 N HCl solution, followed by the addition of ether. The resulting heterogeneous mixture was rapidly stirred for 1 h. The crystals were filtered off, washed with ether, and dried in vacuo for 1 h (0.31 g, 75%).

The following products were prepared in the same manner.

2-(4-Fluorobenzyl)-4,9-dihydroxybenzo[*f*]isoindole-1,3-dione (**7**): 34% yield.

7-(3-Bromobenzyl)-5,9-dihydroxy-2-methylpyrrolo[3,4-g]quinoline-6,8-dione (**8b**): 62% yield, 120 h.

7-(3-Bromobenzyl)-5,9-dihydroxypyrrolo[3,4-g]cinnoline-6,8-dione (**9**): 4% yield.

7-(3-Bromobenzyl)-5,9-dihydroxypyrrolo[3,4-g]quinoxaline-6,8-dione (**10**): 60% yield.

5,9-Dihydroxy-7-methylpyrrolo[3,4-g]quinoxaline-6,8-dione (**11a**): 66% yield.

7-Cyclopentyl-5,9-dihydroxypyrrolo[3,4-g]quinoxaline-6,8-dione (**11b**): 31% yield.

5,9-Dihydroxy-7-piperidin-4-ylpyrrolo[3,4-g]quinoxaline-6,8-dione (**11c**): 78% yield.

7-(1-Benzoylpiperidin-4-yl)-5,9-dihydroxypyrrolo[3,4-g]quinoxaline-6,8-dione (**11d**): 44% yield.

7-Cyclohexylmethyl-5,9-dihydroxypyrrolo[3,4-g]quinoxaline-6,8-dione (**11e**): 13% yield.

5,9-Dihydroxy-7-[(1*R*)-1-phenylethyl]pyrrolo[3,4-g]quinoxaline-6,8-dione (**12a**): 26% yield.

5,9-Dihydroxy-7-[(1*S*)-1-phenylethyl]pyrrolo[3,4-g]quinoxaline-6,8-dione (**12b**): 17% yield.

7-Benzo[1,3]dioxol-5-yl-5,9-dihydroxypyrrolo[3,4-g]quinoxaline-6,8-dione (**13a**): 74% yield.

7-Benzo[1,3]dioxol-5-ylmethyl-5,9-dihydroxypyrrolo[3,4-g]quinoxaline-6,8-dione (**13b**): 55% yield.

7-(2-Benzo[1,3]dioxol-5-ylethyl)-5,9-dihydroxypyrrolo[3,4-g]quinoxaline-6,8-dione (**13c**): 28% yield.

5,9-Dihydroxy-7-(2-methoxybenzyl)pyrrolo[3,4-g]quinoxaline-6,8-dione (**14a**): 81% yield.

5,9-Dihydroxy-7-(4-methoxybenzyl)pyrrolo[3,4-g]quinoxaline-6,8-dione (**14b**): 4% yield.

7-(2,6-Dimethoxybenzyl)-5,9-dihydroxypyrrolo[3,4-g]quinoxaline-6,8-dione (**14c**): 50% yield.

7-(2,3-Dimethoxybenzyl)-5,9-dihydroxypyrrolo[3,4-g]quinoxaline-6,8-dione (**14d**): 23% yield.

7-(2,4-Dimethoxybenzyl)-5,9-dihydroxypyrrolo[3,4-g]quinoxaline-6,8-dione (**14e**): 31% yield.

7-(2,5-Dimethoxybenzyl)-5,9-dihydroxypyrrolo[3,4-g]quinoxaline-6,8-dione (**14f**): 44% yield.

5,9-Dihydroxy-7-(4-methylbenzyl)pyrrolo[3,4-g]quinoxaline-6,8-dione (**15a**): 41% yield.

5,9-Dihydroxy-7-(4-trifluoromethoxybenzyl)pyrrolo[3,4-g]quinoxaline-6,8-dione (**15b**): 15% yield.

5,9-Dihydroxy-7-(4-trifluoromethylbenzyl)pyrrolo[3,4-g]quinoxaline-6,8-dione (**15c**): 29% yield.

7-(3-Fluorobenzyl)-5,9-dihydroxypyrrolo[3,4-g]quinoxaline-6,8-dione (**15d**): 11% yield.

7-(4-Fluorobenzyl)-5,9-dihydroxypyrrolo[3,4-g]quinoxaline-6,8-dione (**15e**): 21% yield.

7-(4-Bromo-2-fluorobenzyl)-5,9-dihydroxypyrrolo[3,4-g]quinoxaline-6,8-dione (**15f**): 57% yield.

7-(5-Bromo-2-fluorobenzyl)-5,9-dihydroxypyrrolo[3,4-g]quinoxaline-6,8-dione (**15g**): 77% yield.

7-(3,5-Difluorobenzyl)-5,9-dihydroxypyrrolo[3,4-g]quinoxaline-6,8-dione (**15h**): 52% yield.

7-(3-Chloro-4-fluorobenzyl)-5,9-dihydroxypyrrolo[3,4-g]quinoxaline-6,8-dione (**15i**): 36% yield.

7-(3-Chlorobenzyl)-5,9-dihydroxypyrrolo[3,4-g]quinoxaline-6,8-dione (**15j**): 54% yield.

7-(4-Chlorobenzyl)-5,9-dihydroxypyrrolo[3,4-g]quinoxaline-6,8-dione (**15k**): 48% yield; LRMS (ES⁺) *m/z* 358 (M + H)⁺; LRMS (ES⁻) *m/z* 356 (M - H)⁻; HPLC (system 1) *t*_R 6.62 min, 98.56%; HPLC (system 2) (286 nm) *t*_R 6.13 min, 98.58%; HPLC (system 3) (288 nm) *t*_R 6.38 min, 96.78%. Anal. Calcd for C₁₇H₁₀ClN₃O₄·0.05H₂O: C, 57.25; H, 2.85; N, 11.78. Found: C, 56.03; H, 2.89; N, 11.33.

7-(3,4-Dichlorobenzyl)-5,9-dihydroxypyrrolo[3,4-g]quinoxaline-6,8-dione (**15l**): 58% yield; ¹H NMR (DMSO) δ 4.84 (s, 2H, C₆H₅CH₂), 7.39 (dd, 1H, *J* = 2.03 and *J* = 8.35, CH_{arom}), 7.66–7.69 (m, 1H, CH_{arom}), 7.69 (s, 1H, CH_{arom}), 9.20 (s, 2H, CH_{arom} (2×)), 11.20–11.50 (brs, 2H, OH (2×)); ¹³C NMR (DMSO) δ 39.9 (CH₂), 109.9 (C_{arom}), 127.8, 129.5 (CH_{arom}), 130.0 (C_{arom}), 130.7 (CH_{arom}), 131.0 (C_{arom}), 138.1, 138.7, 145.1 (C_{arom}), 145.5 (CH_{arom}), 165.2 (CO); LRMS (ES⁺) *m/z* 390 (M + H)⁺; LRMS (ES⁻): *m/z* 388 (M - H)⁻; HPLC (system 1) *t*_R 7.16

min, 98.18%; HPLC (system 2) (293 nm) t_R 6.69 min, 98.56%; HPLC (system 3) (288 nm) t_R 6.96 min, 98.09%. Anal. ($C_{17}H_9Cl_2N_3O_4 \cdot 0.12H_2O$) C, H, N.

7-(3,5-Dichlorobenzyl)-5,9-dihydroxypyrrrolo[3,4-*g*]quinoxaline-6,8-dione (**15m**): 61% yield.

7-(2-Bromobenzyl)-5,9-dihydroxypyrrrolo[3,4-*g*]quinoxaline-6,8-dione (**15n**): 27% yield.

5,9-Dihydroxy-7-pyridin-4-ylmethylpyrrrolo[3,4-*g*]quinoxaline-6,8-dione (**16**): 9% yield.

5,9-Dihydroxy-7-naphthalen-2-ylmethylpyrrrolo[3,4-*g*]quinoxaline-6,8-dione (**17a**): 8% yield.

5,9-Dihydroxy-7-(3-thiophen-2-ylbenzyl)pyrrrolo[3,4-*g*]quinoxaline-6,8-dione (**17b**): 48% yield.

7-(2-Fluorobiphenyl-3-ylmethyl)-5,9-dihydroxypyrrrolo[3,4-*g*]quinoxaline-6,8-dione (**17c**): 39% yield.

7-(2'-Fluorobiphenyl-4-ylmethyl)-5,9-dihydroxypyrrrolo[3,4-*g*]quinoxaline-6,8-dione (**17d**): 41% yield.

7-Biphenyl-4-ylmethyl-5,9-dihydroxypyrrrolo[3,4-*g*]quinoxaline-6,8-dione (**17e**): 19% yield.

5,9-Dihydroxy-7-phenethylpyrrrolo[3,4-*g*]quinoxaline-6,8-dione (**18**): 26% yield.

Reaction Procedures of Heterocycles Diester Analogues (32a–d). Pyridine-2,3-dicarboxylic acid dimethyl ester (32a) was purchased from ABCR.

Synthesis of 6-Methylpyridine-2,3-dicarboxylic Acid Dimethyl Ester (32b). 6-Methylpyridine-2,3-dicarboxylic acid (5.10 g, 28.18 mmol) was dissolved in methanol (80 mL), followed by the addition of 6 N HCl in 2-propanol solution (3 mL). The solution was refluxed for 72 h. The solution was cooled to room temperature and concentrated. The residue was coevaporated with toluene (5.81 g, 99%).

Synthesis of Pyridazine-3,4-dicarboxylic Acid Diethyl Ester (32c). This compound was synthesized according to the procedure described by Vors et al.³²

Synthesis of Pyrazine-2,3-dicarboxylic Acid Dimethyl Ester (32d). Pyrazine-2,3-dicarboxylic acid (21.86 g, 0.13 mol) was dissolved in methanol (400 mL), followed by the addition of 6 N HCl in 2-propanol solution (15 mL). The solution was heated at reflux for 24 h. The residue was evaporated and the residue was dissolved in dichloromethane (50 mL). The organic layer was washed with saturated sodium bicarbonate solution (3 × 50 mL), dried over magnesium sulfate, and evaporated under reduced pressure to yield the title compound (25.48 g, 100%), which solidified on standing.

Molecular Modeling Methods. The A-chain of the trimeric crystal structure with PDB code 1BIU¹⁴ was used as the basis for our docking protocol. The protein surface loop comprised of residues 141–147 is not resolved in this structure. The coordinates of these residues were therefore obtained from the PDB structure with code 1BIS¹⁴ by superimposing the C α atoms of three residues on either side of the gap in the 1BIU structure. At the active site, we added two more water molecules to provide for an octahedral coordination of the Mg²⁺ ion. Hydrogen atoms were added to the structure and a molecular mechanics minimization was carried out with the positions of the C α atoms tethered to their crystal structure coordinates. The enol form of the diketo acid I (Figure 2) was manually positioned into the binding pocket by removing two water molecules from the coordination sphere of the Mg²⁺ ion and replacing these by the keto carbonyl and hydroxy oxygen atoms of the inhibitor. As there are four water molecules and the diketo acid can coordinate adjacent positions of the Mg²⁺ coordination sphere in two ways, there are 10 possible orientations of the inhibitor, most of which severely clash with the enzyme. The configuration shown in Figure 1 is the one with the lowest enzyme–inhibitor interaction after molecular mechanics minimization of the manually constructed complex. The diketo acid was removed from this complex, and the coordinates of the enzyme, Mg²⁺ ion, and its two remaining coordinating water molecules form the binding pocket used in the docking protocol described in the modeling section. Minimization of enzyme–ligand complexes is carried out until the root-mean-square gradient is below 0.05 kcal/mol Å; for ligands and Mg²⁺ chelates, this threshold is 10⁻⁶ kcal/mol Å.

In complex minimizations the C α backbone atoms are tethered to their crystal structure positions with a harmonic potential with a force constant of 10 kcal/mol. Å. All software is developed in-house and is run on a Silicon Graphics Origin 2000 system.

Integrase Activity Assay. The integrase activity was determined using an oligonucleotide-based assay in which the DNA strand transfer by preformed complexes of integrase and processed DNA was measured by means of an ELISA test in microtiter plate format. Recombinant His-tagged HIV-1 integrase was produced in the *Escherichia coli* strain BL21(DE3) from the plasmid pINS.D.His.sol (NIH) as described previously.⁴⁰ HPLC-purified oligonucleotides (Prologo) were used for the preparation of viral DNA substrate and target DNA. INb-1C: 5'-bGTGTGGAAAATCTCTAGCAGT-3', IN-1NC: 5'-ACT-GCTAGAGATTTTCCACAC-3'. INT5: 5'-TGACCAAGGGCT-AATTCACf-3', INT6: 5'-AGTGAATTAGCCCTTGGTCAf-3'. INb-1C is 5'-biotinylated, and INT5 and INT6 are labeled with FITC at the 3'-end. INb-1C and IN-1NC correspond to the U5 end of the HIV-1 LTR. The DNA substrate and target DNA were made by annealing INb-1C and IN-1NC, and INT5 and INT6, respectively. An equimolar mixture of both oligonucleotides was heated shortly at 95 °C in the presence of 100 mM NaCl and allowed to cool slowly to room temperature.

For the integration strand transfer reactions, 20 nM biotinylated DNA substrate was preincubated with 300 nM HIV-integrase at 37 °C for 5 min. Serial dilutions of the compounds and 50 nM target DNA were added to the reaction mix containing 20 mM Hepes pH 7.5, 25 mM NaCl, 5 mM MnCl₂, 2 mM DTT, and 50 μg/mL BSA, and the mixture incubated for 2 h at 37 °C. The reaction mix was transferred to streptavidine-coated plates (NoAb discoveries), which were prewashed with 5× SSCT, and incubated for 1 h at room temperature. Plates were washed with 2× SSCT, anti-FITC POD-coupled antibody (Roche) was added, and the plates were incubated for 1 h at room temperature. After a final washing step with PBST, BM chemiluminescent POD-substrate (Roche) was added, and luminescence was read.

Cell-Based Anti-HIV and Toxicity Assay. The antiviral activity has been determined with a cell-based replication assay. This assay directly measures the ongoing replication of virus in MT4 cells via the specific interaction of HIV-tat with LTR sequences coupled to GFP. In the toxicity assay, a reduced expression of the GFP reporter protein serves as a marker for the cellular toxicity of a compound. Briefly, various concentrations of the test compounds are brought into a 384-well microtiter plate. Subsequently, MT4 cells and HIV-1/LAI (wild type) are added to the plate at a concentration of respectively 150 000 cells/mL and 200 cell culture 50% infectious doses (CCID₅₀). To determine the toxicity of the test compound, mock-infected cell cultures containing an identical compound concentration range are incubated for 3 days (37 °C, 5% CO₂) in parallel with the HIV-infected cell cultures.

On the basis of the calculated percent inhibition for each compound concentration, dose–response curves are plotted and EC₅₀ and pEC₅₀ and CC₅₀ and pCC₅₀ values are calculated.

Acknowledgment. The authors thank Marleen Van Dooren for her analytical support and Marie-Pierre de Bethune, Karen Manson, Frank Daelemans and Gemma Campabadal I Monfà for reviewing the manuscript.

Supporting Information Available: Spectroscopic data for intermediate and final compounds. This material is available free of charge via the Internet at <http://pubs.acs.org>.

References

- Coffin, J. C.; Hughes, S. H.; Varmus, H. E. *Retroviruses*; Cold Spring Harbor Laboratory Press: Plainview, NY, 1999.
- Neamati, N. Patented small molecule inhibitors of HIV-1 integrase: A 10-year saga. *Expert Opin. Ther. Patents* **2002**, *12*(5), 709–724.
- Singh, S. B.; Zink, D. L.; Bills, G. F.; Pelaez, F.; Teran, A.; Collado, J.; Silverman, K. C.; Linghman, R. B.; Felock, P.; Hzauda, D. J. Discovery, structure and HIV-1 integrase inhibitory activities of integracins, novel dimeric alkyl aromatics from *Cytonaema* sp. *Tetrahedron Lett.* **2002**, *43*, 1617–1620.

- (4) Chiu, T. K.; Davies, D. R. Structure and function of HIV-1 integrase. *Curr. Top. Med. Chem.* **2004**, *4*(9), 965–977.
- (5) Anthony, N. J. HIV-1 integrase, a target for new AIDS chemotherapeutics. *Curr. Top. Med. Chem.* **2004**, *4*(9), 979–990.
- (6) Goldgur, Y.; Craigie, R.; Cohen, G. H.; Fujiwara, T.; Yoshinaga, T.; Fujishita, T.; Sugimoto, H.; Endo, T.; Murai, H.; Davies, D. R. Structure of the HIV-1 Integrase Catalytic Domain Complexed with an Inhibitor: A Platform for Antiviral Drug Design. *Proc. Natl. Acad. Sci. U.S.A.* **1999**, *96*, 13040–13043.
- (7) Sotriffer, C. A.; Ni, H.; McCammon, F. A. HIV-1 Integrase Inhibitor Interactions at the Active Site: Prediction of Binding Modes Unaffected by Crystal Packing. *J. Am. Chem. Soc.* **2000**, *122*, 6136–6137.
- (8) Sotriffer, C. A.; Ni, H.; McCammon, F. A. Active Site Binding Modes of HIV-1 Integrase Inhibitors. *J. Med. Chem.* **2000**, *43*, 4109–4117.
- (9) Makhija, M. T.; Kulkarni, V. M. Molecular Electrostatic Potentials as Input for the Alignment of HIV-1 Integrase Inhibitors in 3D QSAR. *J. Comput. Aid. Mol. Des.* **2001**, *15*, 961–978.
- (10) Yuang, H.; Parrill, A. L. QSAR Studies of HIV-1 Integrase Inhibition. *Bioorgan. Med. Chem.* **2002**, 4169–4183.
- (11) Buolamwini, J. K.; Assefa, H. CoMFA and CoMSIA 3D QSAR and Docking Studies on Conformationally-Restrained Cinnamoyl HIV-1 Integrase Inhibitors: Exploration of a Binding Mode at the Active Site. *J. Med. Chem.* **2002**, *45*, 841–852.
- (12) Kuo, C.-L.; Assefa, H.; Kamath, S.; Brzozowski, Z.; Slawinski, J.; Saczewski, F.; Buolamwini, J. K.; Neamati, N. Application of CoMFA and CoMSIA 3D-QSAR and Docking Studies in Optimization of Mercaptobenzenesulfonamides as HIV-1 Integrase Inhibitors. *J. Med. Chem.* **2004**, *47*, 385–399.
- (13) Parrill, A. L. HIV-1 Integrase Inhibition: Binding Sites, Structure Activity Relationships and Future Perspectives. *Curr. Med. Chem.* **2003**, *10*, 1811–1824.
- (14) Goldgur, Y.; Dyda, F.; Hickman, A. B.; Jenkins, T. M.; Craigie, R.; Davies, D. R. Three New Structures of the Core Domain of HIV-1 Integrase: An Active Site that Binds Magnesium. *Proc. Natl. Acad. Sci. U.S.A.* **1998**, *95*, 9150–9154.
- (15) Maignan, S. M.; Guilloteau, J. P.; Zhou-Liu, Q.; Clement-Malla, C.; Mikol, V. Crystal Structures of the Catalytic Domain of HIV-1 Integrase Free and Complexed with its Metal Cofactor: High Level of Similarity of the Active Site with Other Viral Integrases. *J. Mol. Biol.* **1998**, *282*, 359–368.
- (16) Dyda, F.; Hickman, A. B.; Jenkins, T. M.; Engelman, A.; Craigie, R.; Davies, D. R. Crystal Structure of the Catalytic Domain of HIV-1 Integrase: Similarity to Other Polynucleotidyl Transferases. *Science* **1994**, *266*, 1981–1986.
- (17) Lodi, P. J.; Ernst, J. A.; Kuszewski, J.; Hickman, A. B.; Engelman, A.; Craigie, R.; Clore, G. M.; Gronenborn, A. M. Solution Structure of the DNA Binding Domain of HIV-1 Integrase. *Biochemistry* **1995**, *34*, 9826–9833.
- (18) Cai, M.; Zheng, R.; Caffrey, M.; Craigie, R.; Clore, G. M.; Gronenborn, A. M. Solution Structure of the N-Terminal Zinc Binding Domain of HIV-1 Integrase. *Nat. Struct. Biol.* **1997**, *4*, 567–577.
- (19) Cai, M.; Huang, Y.; Caffrey, M.; Zheng, R.; Craigie, R.; Clore, G. M.; Gronenborn, A. M. Solution Structure of the His12 → Cys Mutant of the N-Terminal Zinc Binding Domain of HIV-1 Integrase Complexed to Cadmium. *Protein Sci.* **1998**, *7*, 2669–2674.
- (20) Bujacz, G.; Alexandratos, J.; Qing, Z. L.; Clement-Mella, C.; Wlodawer, A. The Catalytic Domain of Human Immunodeficiency Virus Integrase: Ordered Active Site in the F185H Mutant. *FEBS Lett.* **1999**, *398*, 175–178.
- (21) Eijkelenboom, A. P. A. M.; Sprangers, R.; Hard, K.; Puras Lutzke, R. A.; Plasterk, R. H. A.; Boelens, R.; Kaptein, R. Refined Solution Structure of the C-Terminal DNA-Binding Domain of HIV-1 Integrase. *Proteins: Struct., Funct., Genet.* **1999**, *36*, 556–564.
- (22) Greenwald, J.; Le, V.; Butler, S. L.; Bushman, F. D.; Choe, S. The Mobility of an HIV-1 Integrase Active Site Loop is Correlated with Catalytic Activity. *Biochemistry* **1999**, *38*, 8892–8898.
- (23) Chen, J. C.-H.; Krucinski, J.; Miercke, L. J. W.; Finer-Moore, J. S.; Tang, A. H.; Leavitt, A. D.; Stroud, R. M. Crystal Structure of the HIV-1 Integrase Catalytic Core and C-Terminal Domains: A Model for Viral DNA Binding. *Proc. Nat. Acad. Sci. U.S.A.* **2000**, *97*, 8233–8238.
- (24) Wang, J.; Ling, H.; Yang, W.; Craigie, R. Structure of a Two-Domain Fragment of HIV-1 Integrase: Implication for Domain Organization in the Intact Protein. *EMBO J.* **2001**, *20*, 7333–7343.
- (25) Grobler, J. A.; Stillmock, K.; Hu, B.; Witmer, M.; Felock, P.; Espeseth, A. S.; Wolfe, A.; Egbertson, M.; Bourgeois, M.; Melamed, J.; Wai, J. S.; Young, S.; Vacca, J.; Hazuda, D. J. Diketoacid Inhibitor Mechanism and HIV-1 Integrase: Implications for Metal Binding in the Active Site of Phosphotransferase Enzymes. *Proc. Natl. Acad. Sci. U.S.A.* **2002**, *99*, 6661–6666.
- (26) Neamati, N.; Lin, Z.; Karki, R. G.; Orr, A.; Cowansage, K.; Strumberg, D.; Pais, G. C. G.; Voigt, J. H.; Nicklaus, M. C.; Winslow, H. E.; Zhao, H.; Turpin, J. A.; Yi, J.; Skalka, A. M.; Burke, T. R.; Pommier, Y. Metal-Dependent Inhibition of HIV-1 Integrase. *J. Med. Chem.* **2002**, *45*, 5661–5670.
- (27) Marchand, M.; Johnson, A. A.; Karki, R. G.; Pais, G. C. G.; Zhang, X.; Cowansage, K.; Patel, T. A.; Nicklaus, M. C.; Burke, T. R.; Pommier, Y. Metal-Dependent Inhibition of HIV-1 Integrase by Diketoacids and Resistance of the Soluble Double-Mutant (F185K/C290S). *Mol. Pharmacol.* **2003**, *64*, 600–609.
- (28) Wai, J. S.; Egbertson, M. S.; Payne, L. S.; Fisher, T. E.; Embrey, M. W.; Tran, L. O.; Melamed, J. Y.; Langford, H. M.; Guare, J. P.; Zhuang, L.; Grey, V. E.; Vacca, J. P.; Holloway, M. K.; Naylor-Olsen, A. M.; Hazuda, D. J.; Felock, P. J.; Wolfe, A. L.; Stillmock, K. A.; Schleif, W. A.; Gabryelski, L. J.; Young, S. D. 4-Aryl-2,4-dioxobutanoic Acid Inhibitors of HIV-1 Integrase and Viral Replication in Cells. *J. Med. Chem.* **2000**, *43*, 4923–4926.
- (29) Fikkert, V.; Van Maele, B.; Vercammen, J.; Hantson, A.; Van Remoortel, B.; Michiels, M.; Gurnari, C.; Pannecouque, C.; De Maeyer, M.; Engelborghs, Y.; De Clercq, E.; Debyser, Z.; Witvrouw, M. Development of Resistance against Diketo Derivatives of Human Immunodeficiency Virus Type 1 by Progressive Accumulation of Integrase Mutations. *J. Virol.* **2003**, *77*, 11459–11470.
- (30) Young, S. D.; Egbertson, M.; Payne, L. S.; Wai, J. S.; Fisher, T. E.; Guare, J. P.; Embrey, M. W.; Tran, L.; Zhuang, L.; Vacca, J. P.; Langford, M.; Melamed, J.; Clark, D. L.; Medina, J. C.; Jean, J. Preparation of aromatic and heteroaromatic 4-aryl-2,4-dioxobutyric acid derivatives useful as HIV integrase inhibitors. PCT Int. Appl. WO 9962520 A1, 1999.
- (31) Kabsch, W. A Discussion of the Solution for the Best Rotation to relate two Sets of Vectors. *Acta Crystallogr.* **1978**, *A34*, 827–828.
- (32) Halgren, T. A. Merck molecular force field. I. Basis, form, scope, parametrization and performance of MMFF94. *J. Comput. Chem.* **1996**, *17*, 490–519.
- (33) Daeyaert, F.; De Jonge, M.; Heeres, J.; Koymans, L.; Lewi, P.; Vinkers, H. M.; Janssen, P. A. J. A Pharmacophore Docking Algorithm and its Application to the Cross-Docking of 18 HIV-NRTI's in their Binding Pockets. *Proteins* **2003**, *56*, 526–533.
- (34) Hazuda, D. J.; Young, S. D. Inhibitors of human immunodeficiency virus integration. *Adv. Antiviral Drug Des.* **2004**, *4*, 63–77.
- (35) Katoh, S.; Miyazaki, S.; Habuka, N. Preparation of β -Ketoamide Compounds as HIV Integrase Inhibitors. WO 2003016266, 2003.
- (36) Pais, G. C. G.; Burke, T. R., Jr. Novel aryl diketo-containing inhibitors on HIV-1 integrase. *Drugs Future* **2002**, *27*(11), 1101–1111.
- (37) Vors, J.-P. A convenient Synthesis of Pyridazine-3,4-dicarboxylic Acid by a Hetero Diels–Alder Reaction. *J. Heterocycl. Chem.* **1990**, *27*, 579–582.
- (38) Murray, W. M.; Semple, J. E. Facile Access to Novel 1,4-Dihydroxynaphthalene-2,3-dicarboximides and Heterofused analogues. *Synthesis* **1996**, 1180–1182.
- (39) Young, S. D.; Anthony, N.; Wai, J.; Fisher, T.; Zhuang, L.; Embrey, M.; Egbertson, M.; Payne, L.; Melamed, J.; Langford, M.; Kuo, M.; Gomez, R.; Jolly, S.; Guare, J.; Vacca, J.; Huff, J.; Jin, L.; Ciecko, P.; Lin, J.; Yergey, J.; Wong, B.; Chen, I. W.; Pearson, P.; Petropoulos, C.; Heilock, G.; Parkin, N.; Kemp, R.; Vargas, H.; Sigel, P.; Bunting, P.; Galloway, S.; Summa, V.; Rowley, M.; Gardelli, C.; Pace, P.; Felock, P.; Wolfe, A.; Stillmock, K.; Witmer, M.; Miller, M.; Blau, C.; Espeseth, A.; Cole, J.; Grobler, J.; Schleif, W.; Moyer, G.; Gabryelski, L.; Emini, E.; Hzauda, D. L-870,810: Discovery of a Potent HIV Integrase Inhibitor with Potential Clinical Utility. XIV International AIDS Conference, Barcelona, abstract LbPEA9007, 2002.
- (40) Jenkins, T. M.; Engelman, A.; Ghrilando, R.; Craigie, R. A Soluble Active Mutant of HIV-1 Integrase Involvement of Both the Core and Carboxyl-Terminal Domains in Multimerization. *J. Biol. Chem.* **1996**, *271*, 7712–7718.

JM049559Q